



This is a repository copy of *MET-IRSL used to track pre-depositional sediment transport history*.

White Rose Research Online URL for this paper:

<https://eprints.whiterose.ac.uk/188132/>

Version: Accepted Version

Article:

Rhodes, E.J. orcid.org/0000-0002-0361-8637 and Leathard, J.A. (2022) MET-IRSL used to track pre-depositional sediment transport history. *Quaternary Geochronology*, 70. 101294. ISSN 1871-1014

<https://doi.org/10.1016/j.quageo.2022.101294>

© 2022 Published by Elsevier B.V. This is an author produced version of a paper subsequently published in *Quaternary Geochronology*. Uploaded in accordance with the publisher's self-archiving policy. Article available under the terms of the CC-BY-NC-ND licence (<https://creativecommons.org/licenses/by-nc-nd/4.0/>).

Reuse

This article is distributed under the terms of the Creative Commons Attribution-NonCommercial-NoDerivs (CC BY-NC-ND) licence. This licence only allows you to download this work and share it with others as long as you credit the authors, but you can't change the article in any way or use it commercially. More information and the full terms of the licence here: <https://creativecommons.org/licenses/>

Takedown

If you consider content in White Rose Research Online to be in breach of UK law, please notify us by emailing eprints@whiterose.ac.uk including the URL of the record and the reason for the withdrawal request.



eprints@whiterose.ac.uk
<https://eprints.whiterose.ac.uk/>

MET-IRSL used to track pre-depositional sediment transport history

Rhodes E. J.^{*a,b} and Leathard J. A.^a

^aDepartment of Geography, University of Sheffield, Western Bank, Sheffield, S10 2TN, UK

^bEarth, Planetary, and Space Sciences, University of California Los Angeles, 595 Charles Young Drive East, Los Angeles, CA 90095-1567, USA

* Corresponding author.

E-mail address: ed.rhodes@sheffield.ac.uk (E.J. Rhodes).

Keywords: MET-IRSL, Photochronometry, Sediment transport, glacial

Author accepted manuscript, published as Quaternary Geochronology 70, May 2022, 101294, <https://doi.org/10.1016/j.quageo.2022.101294>

Abstract

This paper explores a series of single grain MET-IRSL (multiple elevated temperature infrared stimulated luminescence) determinations undertaken in order to assess the potential of this approach, developed over the last decade and previously applied to a range of applications, in determining how eroded material moves through environments. Three different approaches are explored here, namely: i) an assessment of the potential to use the technique for improving the robustness of IRSL or P-IR-IRSL age estimates by identifying only well-bleached grains, ii) a means to characterise patterns of grain transport within a catchment using a newly established parameter, the “burial-bleach ratio”, and iii) a novel proxy that responds to changes in light availability through time, here referred to as palaeophotochronometry. For the second approach that we explore, a direct comparison of the MET-IRSL results from several sites with particle size analysis (PSA) data for the same sediment is included. This comparison highlights striking similarities between dispersal of single grain (SG) MET-IRSL burial-bleach ratio data and PSA distributions for some samples, suggesting that we may be able to place a timescale on the acquisition of this fundamental sedimentary characteristic. Common to these three SG MET-IRSL approaches is the importance of characterising and interpreting the previous bleaching records for individual grains.

1.0 Introduction

Multiple elevated temperature (MET) IRSL measurements can be useful in several ways, as the different charge populations that are accessed by a series of IRSL measurements performed at increasing temperatures display a range of both thermal stabilities and optical sensitivity (or bleachability). This provides the opportunity to assess signal stability or complete zeroing when dating sediments (Li and Li, 2011; Reimann et al., 2015), for application as a multi-stability low temperature thermochronometer (King et al., 2016), and as a tool to study sediment transport based on differential signal bleaching characteristics (McGuire and Rhodes, 2015a, b; Gray et al., 2017).

Here we assess the extension to further applications including i) identification of full bleaching in the dating of single grains from sediments in a glacial context, building on the approach of Reimann et al. (2015), ii) use of the newly defined parameter “burial-bleach ratio” as a means to characterise sediment transport patterns, and iii) variations in the degree of bleaching through time experienced by individual grains within a single sample, here termed palaeophotometry. In all three of these applications, the variation in bleaching for the different feldspar MET-IRSL signal components is the main characteristic of that is drawn upon. Below we present observations, and consider possible limitations, including systematic effects such as first cycle sensitivity change, thermal transfer and the presence of noise superimposed on an environmental signal.

Different temperature MET-IRSL signals within a single sample or grain are bleached by light exposure at different rates, allowing us to interpret two signals from the same grain displaying the same equivalent dose as an indication that both signals were most likely adequately zeroed at the time of deposition (Fig. 1a). This interpretation is consistent with other forms of plateau method widely used in luminescence dating (example reference; Li and Li, 2011), and was the basis of the adequate bleaching assessment of Reimann et al. (2015). Below, we explore the use of plateau “depth”, that is which MET-IRSL signals are included within the observed plateau, as a first-order method to assess ancient relative light exposure; grains bleached for longer times will have higher temperature MET-IRSL signals more fully reset, so have more extensive or “deeper” plateaux, in some cases extending to the 230°C signal, the highest temperature MET-IRSL measured in this study. We refer to this degree of bleaching as a palaeophotometry index, and we show how this can vary through time for one of our samples. We discuss possible limitations to this approach, including specific problems relating to poor dose recovery for the highest temperature MET-

IRSL signal measured in some samples, along with the significance of these preliminary results.

We observe that many grains provide apparent age estimates for different MET-IRSL signals but do not display a plateau (e.g. Fig. 1b). That is, the age estimates (or equivalent dose values) are not in agreement within their measurement uncertainties. However, these grains can still provide valuable information about past light exposure, as the gradient of the increase in apparent age (as a function of the characteristic bleach time for each signal) relates to longer term signal growth during burial and loss during bleaching episodes. We establish a parameter we call burial-bleach ratio (B-B ratio) based on this gradient, and show how these values can provide information about grain transport dynamics and depositional environments.

Fig. 1 here

1.1 Sample locations

Sample sites selected include an ice-marginal delta formed with an ice-dammed glacial lake that existed during the last glacial cycle around the time of the last glacial maximum (LGM). This site is in Chinley, Derbyshire, UK, and is described by Delaney et al. (2010) and Jowett and Charlesworth (1929); reconstruction of the BIIS (British and Irish Ice Sheet) by the BriticeChrono team places the delta constructional age range as 28-24ka (Chiverrell et al., 2020), with the end of this period considered the most likely date during ice recession from the Goyt Valley associated with falling lake levels (Delaney et al., 2010). Three closely spaced samples were collected in a small cleaned vertical exposure located in Brownside, a region of Chinley, in 2016; one sample was in horizontally bedded sands interpreted as delta top sets (field code BS16-01, laboratory code Shfd 16132), and below this two further samples, BS16-02 (Shfd 16133) very close beneath the topsets in dipping delta foresets, and BS16-03 (Shfd 16134) around 10cm lower also in foresets, dipping at about 17° towards the SE, away from the inferred ice-margin.

Several samples were collected from Ilkley Moor, Yorkshire, UK, in two batches. The first collection targeted sandy deposits of unknown origin positioned stratigraphically beneath peat at the edge of Crawshaw Moss, the site for the research project "Oasis in the desert?" led by Swindels, Payne and Mallon. These three samples (field codes IM19-01, IM19-02, IM19-03 with laboratory codes 20040, 20041, 20042 respectively) were collected in order to determine their genesis, and the sedimentary environments pertaining at the time of

deposition. A second group of samples included modern fluvial sands from Black Beck, the small stream that drains Crawshaw Moss. These included a stranded sand unit deposited during an earlier high flow event located approximately 10cm above the stream surface (field code IM19-05, Shfd 20128), and a coarser sand from the base of the active channel collected beneath the stream surface (IM19-06, Shfd 20129). Also collected and measured were two sandstone cobbles from the same location, selected to represent bedrock (IM19-R01, Shfd 20160; IM19-R02, Shfd 20161).

In order to provide comparisons with the three Ilkley Moor samples of unknown origin, six samples from three different environments were measured. These included the two fluvial sands from Black Beck described above, two wind-blown (aeolian) dune sands from Twigmoor Woods, Lincolnshire, UK (Bateman et al., 1999; samples TW20-03, Shfd 20158; TW20-04, Shfd 20159), and two glacial sediments exposed within Borrass Quarry, Wrexham, Wales, UK (Chiverrell et al., 2020), comprising a till (BQ20-02, Shfd 20029) and a glacial outwash gravel (BQ20-03, Shfd 20030).

2.0 Methods

2.1 Collection

Samples were collected in metal tubes pushed or hammered into an excavated vertical section; in most cases the sandy sediment sampled was unconsolidated. Following tube removal, an in-situ NaI gamma spectrometer measurement was performed. An additional sample was collected for moisture content analysis. Cobble-sized rock samples from Ilkley Moor were labelled and simply lifted from their original locations at the side of Black Beck.

2.2 Particle size analysis

A fundamental property of any particle is its size, and particle size analysis (PSA) is a well-established proxy technique for determining the environmental deposition of sediment (Sun et al., 2002). These properties affect sediment entrainment, transportation and depositional processes, and the particle size distribution can indicate likely depositional environments. Samples for hand sieving PSA were dried at 40°C, gently disaggregated and subsequently sieved, using a mechanical agitator, following Gale and Hoare (2011). Lower grain sizes were hydrated with hexametaphosphate (0.1%) to homogenise and disaggregate the samples, which were then inserted into a Horiba LA950 laser diffraction particle size analyser.

2.3 IRSL sample preparation

Following extraction from collection tubes and removal of exposed sediment from tube ends under laboratory lighting, each sample was initially treated with dilute HCl to remove carbonate and subsequently H₂O₂ to remove organic material. Rock samples of gritstone (coarse angular sandstone) were sprayed with black paint, and their outer surfaces removed with a hammer and chisel under laboratory lighting. Individual grains were disaggregated using a small hand mill; subsequent treatments for rock samples followed those for other samples. After rinsing and drying, samples were sieved to isolate either 125-180µm or 180-212µm grains; this fraction was density separated using a sodium polytungstate solution at 2.58 g.cm⁻³ to isolate potassium-rich alkali feldspar grains within the material that floated. For IRSL measurement, prepared grains were sprinkled onto Risø single grain mounts, and excess grains carefully brushed off under a binocular microscope using dim amber illumination. Sample holders were placed directly into an automated Risø DASH TL-DA-20D single grain reader fitted with a dual laser single grain XY box.

2.4 IRSL measurement

The single grain MET-IRSL measurement protocol applied was almost identical to that developed by McGuire and Rhodes (2015b), using a preheat of 60s at 250°C, and 2.5s 90% power IR laser illuminations at each of five temperatures, namely 50, 95, 140, 185 and 230°C. A test dose of approximately 8Gy was applied, and then the same preheat treatment (60s at 250°C), followed by an identical IRSL measurement series at the five temperatures listed above. Each SAR cycle ended with a hot bleach, comprising a 100s IRSL exposure using LEDs at 90% power at 290°C (Table 1). Growth curves included a zero dose point, and doses from 6.4Gy up to around 640Gy. Single grain bleaching of the different MET-IRSL signals using blue LEDs was conducted within the reader for some samples following construction of the regenerative growth curves. At the end of the measurement sequence we irradiated and preheated each set of grains; these were stored and subsequently measured using a single SAR cycle that starts with the lowest temperature MET-IRSL measurement in order to explore fading behaviour for each grain. This measurement protocol was validated using dose recovery experiments conducted using multiple grain aliquots (see supplementary material).

Table 1 here

2.5 Analysis

Individual growth curves were fitted using either a single exponential or exponential plus linear function within Analyst 4.57 software. After preliminary identification, a formal assessment of D_e value agreement was made using a statistical test developed from that used in the post-IR IRSL single grain determination described by Rhodes (2015). A nominal low overdispersion value of 0.1% was added in quadrature. This procedure identified two or more D_e values that represent a single bleaching event, subsequently referred to as “plateau” values; on the spreadsheet these were colour coded. Values that did not overlap, but where the D_e value rose with higher MET-IRSL measurement temperature are considered to result from incomplete bleaching, fading, or problems with sensitivity correction (see discussion below). Where several values rise across more than two temperatures, these signals can provide information about multiple bleach and burial cycles; a different colour was used to highlight these values. Finally, we observe for some grains that we have apparently anomalous results where higher temperature MET-IRSL signals provide lower D_e values than measured at a lower temperature for that grain; possible causes of this effect are discussed below.

In order to study patterns of grain transport and storage over several cycles prior to final deposition we estimate a parameter that we refer to as the “burial-bleach ratio”; this represents the gradient of a linear fit to all the apparent MET-IRSL age estimates that were determined for that grain; the y-axis of this plot is age, while the x-axis represents a nominal “bleaching reference time” that is a characteristic of the MET-IRSL signal at that particular temperature (Fig. 2). Note, in the discussion section we point out that bleaching rate varies between samples and individual grains, but this may also depend on past dosing and bleaching history. In principle, it is possible to determine characteristic bleach times for every grain individually, and in fact many of the MET-IRSL measurement sequences used for these samples did include a blue light bleaching treatment spanning four orders of magnitude of exposure time for every grain. This series of measurements is described in the next paragraph. However, we find that many grains that provide adequate age estimates (those with useful D_e values, that is those with reasonable precision and hence meaningful apparent age estimates) display bleach data with a large amount of noise. This is owing to

the MET-IRSL signal reduction that results from bleaching; the small residual IRSL signals at longer exposure times have relatively larger fractional uncertainties than the growth curve data for the same grain. For this reason, we here use aggregated blue light bleach data from a reference sample to determine the bleaching reference times, based on signals reduction of regenerated MET-IRSL signals following 1, 10, 100, 1,000 and 10,000s exposure to blue LEDs (at 90% power); these LEDs are used for conventional multiple grain OSL and illuminate all grains held in a single grain holder at the same time. Note that this procedure is possible in our Risø DASH reader that includes an automated filter changer, but would not be possible to undertake in this efficient manner in a conventional reader owing to filter breakthrough to the PMT from the blue LEDs. The rate of bleaching with blue LEDs at 90% power in the reader used is approximately equal to that under natural Californian sunlight as observed by McGuire and Rhodes (2015a); for example, for the 140°C MET-IRSL signal, the Californian fluvial sample displayed a remnant signal of 21% following 10,000s of natural sunlight exposure, while a Scottish fluvial sample had a remnant signal of 22% for this signal after 10,000s of blue LED exposure. This treatment is intended only as a relative bleaching assessment tool, and not as a response to natural daylight exposure, and is administered following the completion of the regenerative dose treatments to determine equivalent dose. In order to improve counting statistics, a relatively large dose of around 100Gy was given at the start of each bleaching and measurement SAR cycle, followed by the blue LED bleach treatment (0, 1, 10, 100, 1,000, 10,000s in turn), a standard preheat and then the different SG MET-IRSL measurements; as in the standard SG MET-IRSL determination these are followed by a test dose, PH (60s at 250°C), the five MET-IRSL steps, and a final hot bleach of 100s IRSL at 290°C.

3.0 Results

The samples presented in this paper all provided multiple grains that displayed MET-IRSL signals at different temperatures. Those from the Chinley Brownside glacial delta displayed impressively high yields (yield here refers to the proportion of grains that produce at least one meaningful equivalent dose estimate); between 90 and 95% of grains provided an apparent age estimate for at least one MET-IRSL signal. The windblown dune sands from Twigmoor Woods also provided many estimates (~90% yield), while the samples from Ilkley Moor provided fewer results. Fluvial and bedrock samples from Ilkley Moor displayed yields of between 18 and 48%, while the samples of unknown origin from that site had yields ranging from 24 to 62%. The two glacial samples from Borrass Quarry had yields of 70 and 75%.

IRSL signals measured at 50°C were in general more sensitive than those at higher temperatures, but are considered likely to suffer from fading of the trapped charge responsible as this is basically the widely studied IR-50 signal (Lamothe et al., 2003). Observations of results from Chinley appear to confirm this expectation; many grains that provided MET-IRSL plateau age estimates that were consistent with other grains and our independent age control displayed lower apparent ages for the IR-50 signal, in some ways similar to findings of Li et al. (2014). Note that our plateau method automatically excludes these results when only one signal is affected. The degree of saturation at different MET-IRSL measurement temperatures was investigated for Ilkley Moor rock sample 20160 using the “sum all grains” function in analyst, providing a virtual aliquot comprising the sum of signals of all grains on a single holder; signals from the two aliquots of this sample displayed differences in fading behaviour, but most signals were fully in, or very close to, saturation. Exceptions include the 50°C signal from one disc (D_e value ~400 Gy, ~50% of saturation intensity), and the 230°C signal from the other disc (D_e value ~90 Gy, ~90% of saturation intensity); we discuss these observations below. In many samples including those presented in this paper, the 230°C signal displays unexpected or problematic behaviour. This effect has also been observed in the MET-IRSL responses for other samples not described here. This can include a D_e value lower than that measured at lower temperatures, a strikingly low D_0 value, and in some cases growth curves decreasing at high regenerative doses, probably relating to problems with sensitivity correction. For many grains, however, the 230°C signal is included in a plateau with signals from several other temperatures; in those cases it would appear coincidental that the 230°C signal should provide a result in agreement with the other signals by chance, and on balance it seems likely that for many of these grains the 230°C signal is providing a meaningful age estimate. At other temperatures, apparent dose values for some grains appear out of line with others, for example providing lower dose estimates than those observed at lower temperatures, or higher dose values than observed at higher temperatures. These observations are discussed further below.

We assessed the depositional age of the three glacial delta samples from Chinley by identifying the shared minimum apparent age based only on MET-IRSL plateau ages; results are summarized in Figure 2 and Table 2, and the combined values for each sample provide age estimates that range between 21 and 24 ka, consistent within dating uncertainties with the chronological constraints for this site. Note that we initially measured each sample using 125-180 μm K-feldspar grains, but we also re-measured the first sample using 180-212 μm grains (subsample 16132b), providing four different age estimates. Using the discrete minimum age procedures developed for post-IR-IRSL₂₂₅ dating (Rhodes, 2015) we find a

coherent set of age estimates. We excluded two results that come from a single grain that displayed two low value plateaux for sample 16132b, treating these isolated age estimates as outliers in a manner similar to that used in post-IR-IRSL₂₂₅ dating (e.g. Zinke et al., 2017); below we discuss different possible causes of apparent age underestimation. But with the exception of this one grain, 45 plateau results provide apparently consistent age estimates, despite potentially very little light exposure expected at the time of deposition.

Fig. 3 here

Table 2 here

For the samples from Ilkley Moor, besides depositional age, we are concerned with patterns of grain movement prior to final deposition, so the rising D_e estimates (and apparent ages) are of particular interest here. Six “calibration samples” from different depositional environments were also measured in order to assist in the interpretation of the measured signals, including two modern fluvial samples collected on Ilkley Moor itself, two dune samples representing aeolian transport from Twigmooor Woods, and two samples from a sequence of glacial tills and glacial outwash sediments from Borrass Quarry, Wrexham. We observed that the distributions of burial-bleach ratio (or gradient) for the six “calibration” samples (glacial, aeolian and fluvial) bear a striking resemblance to the particle size analysis results from the same samples; these are presented in Fig. 4. We also plot the burial-bleach ratios and PSA distributions for the three “unknown origin” samples from Ilkley Moor (Fig. 4 g, h, i).

Fig. 4 here

The effective zeroing by light of a signal provides an assessment of the minimum daylight exposure required to bleach that MET-IRSL signal. In this way, shared apparent ages for a single grain identified as a plateau value therefore also potentially provides an estimate of how much light exposure was experienced at that event. Using this approach, there is the possibility to investigate changing light exposure (and therefore possibly varying transport processes) or sample characteristics at different times in the past. To undertake this analysis efficiently, we require a sample that comprises grains that experienced remobilization at many different times in the past, and has a high yield. One of our Twigmooor Woods aeolian dune samples (TW20-04, Shfd 20159) displays these characteristics, and we are able to plot a record of changing bleaching extending from the late glacial through the Holocene (Fig. 5). This plot used a simple bleaching index rather than attempting to quantify exposure times

precisely. We note several episodes of reduced light exposure, and have constructed boundary lines, in some ways similar to zone boundaries used in pollen analysis, to mark the beginning and end of the Younger Dryas cold period (Dansgaard et al., 1989). Note our discussion below as to the veracity of these findings, about the effects of random signal variation, and the significance of these findings.

Fig. 5 here

4.0 Discussion

The dating of the first site, a glacial lake delta samples from Chinley Brownside, Debryshire, UK represents an assessment of the potential of MET-IRSL for sediments where incomplete signal zeroing is expected, and extends the work of Smedley et al. (2013; 2015; 2019), Reimann et al. (2012; 2015) and Fu and Li (2013). These samples provided broadly consistent dose recovery results with the protocol used (Figure S1) but assessing the adequacy of full age estimates tests all parts of the dating system. By isolating only age estimates shared by two or more MET-IRSL signals within the same grain, that is those signals displaying a plateau, these samples provide dates broadly consistent with the age constraints provided by the reconstruction of the ice sheet development and recession at around 24-28 ka performed by the BritIceChrono group (Chiverrell et al., 2020). The MET-IRSL ages measured are slightly lower than the expected ages, but close to the lower age of the control, at 24 ka; two values are fully consistent (16132, 16134) while the other two determinations (16132b, 16133) are consistent with 24ka at 2 sigma (Table 2).

We note that age estimates based solely on the top two MET-IRSL signals may suffer from an effect induced for the highest signal caused by irregular sensitivity change, and in some cases may represent a measurement artefact rather than a meaningful age (Kars et al., 2014); for these glacial lake samples we carefully examined how many of the observed 604 plateau ages (from 800 grains measured) involve only the two highest signals, and discovered this was 20, representing 3.3%. None of these plateaux was included in the ages presented here (Figure 3; Table 2) as all provided significantly older age estimates. We also note that these samples did not display a drop in recovered dose values for this highest temperature (Figure S1); but add a caveat that this effect should be considered and looked for when applying MET-IRSL ages.

The geometry of the geomorphic feature sampled, an ice-marginal delta, suggests that construction was by deposition of sediment transported beneath or within the ice into the

lake; the observed dip of foreset beds is consistent with this hypothesis, as these units dip away from the reconstructed ice margin position (Delaney et al., 2010). Under these circumstances, it is perhaps slightly surprising, but reassuring, to observe that such a relatively large number of grains display plateaux at the common minimum age, that is agreement between the apparent age estimates from different MET-IRSL ages for the same grain. In total 45 plateaux were observed in the four sets of measurements that were consistent with the minimum age values determined from these three samples, a total of 800 grains measured (representing approximately 5%). We conclude from this investigation that there are no signs of incomplete zeroing biasing the measured ages towards an overestimate, and that the plateau method has successfully filtered the results to leave only those that were acceptably zeroed with respect to the signals measured within the measurement uncertainties.

In assessing whether results from different MET-IRSL signals for a single grain are mutually consistent within their measurement uncertainties, we assume that both signals have an identical dose rate. We have also assumed that there is little other “disturbance” to the quality of these D_e determination, and have used an overdispersion or σ_b value at this point of just 0.1% (as a place holder effectively representing 0%). This ignores possible failures of the SAR protocol to work perfectly (e.g. Kars et al., 2014; Colarossi et al., 2018), and in the future, it may be appropriate to allow a slightly larger overdispersion value at this stage, perhaps 5 to 10%. However, using this conservative approach, we appear to have achieved effective isolation of the target population, those grains zeroed during transport into the deposit sampled, or very shortly before that. We note that the above mentioned authors have proposed improvements to post-IR-IRSL or MET-IRSL protocols to overcome issues of sensitivity change and charge carry-over including higher test dose values and extended shining before test dose application, and the present authors advocate incorporation of similar modifications into future MET-IRSL protocols.

We can also examine these plateau age results to discover how well these grains were bleached during transport. Using the index developed for photochronometry (Fig. 2), we can assign these glacial delta samples each an average score based solely on the grains that contribute to their age estimates. These grains are surprisingly well bleached with bleaching indices ranging from 2.8 (BS16-01, 16132b 180-212 μ m grains) to 3.6 (BS16-02, 16233); this index can range from a minimum of 1.0 to a maximum value of 4.0. As the sedimentary and geomorphic geometry here suggests transport under ice, this may suggest that well-zeroed grains were washed into the englacial or subglacial fluvial system from the surrounding higher ground, specifically the hills that border the Goyt Valley that would have been ice-free

at this time. Other aspects of the MET-IRSL signals from these samples may provide further clues to their pre-deposition transport in the future, but these questions go beyond the scope of the present research.

We conclude from this part of our study that the MET-IRSL plateau method has the potential to isolate age estimates that represent true bleaching events rather than simply residual signals that were partially reduced by light exposure. Events older than the last deposition, preserved when some grains see very little light during subsequent transport episodes, may represent a valuable source of information regarding past events in that catchment.

When a grain is first eroded from bedrock, its MET-IRSL signals are mostly close to saturation or in steady state; this assumption was broadly confirmed by the investigation into the two rock samples (20160, 20161) from Ilkley Moor. Some signals may be in steady state, below saturation, and provide an opportunity to assess fading (e.g. Brown et al., 2015), though we did not find patterns of consistent signal loss; one virtual aliquot of 100 grains of sample 20160 displayed fading (or possibly adverse sensitivity change) of the 50°C signal, while the other did not. This aspect of MET-IRSL signals would benefit from further study that reaches beyond the scope of the present research. When grains close to saturation are exposed to daylight, the different MET-IRSL trap populations will be reduced at different rates, providing an opportunity to assess exposure duration. However, when grains are again buried, signals still close to saturation will grow at a lower rate than those that were more completely bleached. Over several cycles of burial and bleaching, the ratios of the different MET-IRSL can evolve away from those defined by the bleaching characteristics alone. That is, when a single bleaching event takes place from a well-defined uniform state for the different MET-IRSL populations, only certain ratios of apparent dose (or apparent age) are possible, prescribed by the different bleaching responses for those signals. But when burial episodes are also considered, a wider array of possible apparent age values can be achieved by an individual grain.

Over a period of time, repeated exposures of similar types (intensity, incident wavelengths and duration) can lead to a pattern of increasing age vs signal characteristic bleach time t_b for the MET-IRSL signals of that grain that is either steep or gentle (Fig. 2). The gradient of this slope relates in general terms to the ratio of time spent buried to the time spent exposed to light. While buried, IRSL signal sizes increase as do apparent ages, but time spent exposed to daylight reduces signals and apparent ages, but at very unequal rates with low temperature MET signals being reduced much more rapidly than higher temperature signals (Smedley 2015; Rui et al., 2015). In this way, the gradient of the line in these plots relates to

the ratio of time spent buried vs time spent exposed. More burial equates to steeper gradient, or greater burial-bleach ratio. For these samples, we have not estimated actual burial or bleach times; calculations for other samples suggest that when the ranges of typical burial times are in thousands of years, exposure times that lead to this type of response are of the order of tens of seconds. These considerations and detailed modelling of this effect go beyond the scope of this paper, and here we simply determine the mean gradients on plots similar to Fig. 2, and term this burial-bleach ratio. For this simple treatment, we consider the burial-bleach ratio a potentially useful parameter to determine, and have explored distributions of these values. We note that the characteristic bleach time for each signal used to calculate the burial bleach ratio value is merely a first order value, and that these ratios are intended primarily for use in a relative sense; significant variation in actual bleach times likely exist between different grains and for samples with different origins. This issue requires further research to develop different aspects of photochronometry; the authors note that in most cases, bleaching conditions (e.g. water depth, daylight or sunlight intensity) cannot be reconstructed, so all bleaching time estimates refer to equivalent times of a notional light intensity and quality.

When plotting distributions of burial-bleach (B-B) ratio estimated as described above, we observed that for some samples there appears to be some similarity with the particle size analysis distribution for the same sample. We plot the two parameters side-by-side in Fig. 4 in order to allow direct comparison for our six calibration samples as well as the three samples from Ilkley Moor of unknown depositional environment.

A striking similarity between the two distributions exists for some samples. For the six calibration samples in the upper part, those with wide distributions in PSA tend to have a wide distribution in the B-B ratio, and vice versa. The relationship is between coarser grain sizes and higher burial-bleach ratios. This appears to make sense and match expectation; higher energy systems generally have poorer bleaching, consistent with observations here. These findings suggest to the present authors that we have the prospect of determining aspects of the timescales of PSA characteristics. In the plots constructed to determine B-B ratios, the y-axis is apparent age, providing an element of timescale to this comparison. However, it is considered likely from modelling of other samples that these characteristics develop over multiple transport cycles associated with alternating periods of burial and daylight exposure during movement. Characteristics of these storage and transport cycles, possibly including information concerning their stability, is encoded in the detail of these apparent age vs MET signal responses. Many aspects of observed natural MET-IRSL signals can be reproduced by a simple burial-bleach model that uses values based on real

samples to simulate signal loss and growth. However, this is complex, and lies beyond the scope of the present research. However, such models do offer the prospect of tracing the acquisition of PSA characteristics through inverse modelling of this type of B-B ratio for samples where a close relationship between the two exists. A model allowing “acceleration”, both positive and negative, of both bleach duration and storage duration was found able to simulate a wide range of different MET-IRSL signal values, similar to those observed for real samples such as those presented here, using just five cycles of burial and bleaching.

PSA is considered a powerful tool to assist sedimentologists interpret aspects of sedimentary environments, transport and provenance (Lopez, 2017). We tentatively suggest that B-B ratios may have similar potential, with the added benefit of providing timescale information.

When grains are exposed to light for an extended period, several MET-IRSL trap populations may be reduced to a similar low level close to zero. Following signal growth during burial, they each trap charge and will provide a similar apparent age when the grain is measured. This condition provides a plateau, similar apparent ages for signals of different bleachability; these were used to estimate ages for the glacial delta samples dated above (Figure 3; Table 2). The degree of penetration of the plateau into the harder to bleach IRSL signals provides information concerning the relative intensity of the light exposure. In principle, it may be possible to recover these values in seconds of equivalent exposure, but wide variations in single grain bleaching rates observed suggest that these would not be reliable unless individual bleaching rates are used for each signal for every grain; even if this is done, natural bleaching behaviour may differ to that determined following a dating protocol for the same grain, as charge stores that can reduce bleaching rate by transfer or carry-over processes (e.g. Colarossi et al, 2018) may have been depleted during high temperature bleach or thermal treatments. While we have the potential to perform this type of analysis, as we measured the bleaching behaviour for every grain for several samples, we have not yet undertaken it. In order to assess the potential of this type of analysis, we instead have simply coded the degree of bleaching of plateau events using a simple index. Where only the lowest two signals (50 & 95°C) were bleached, this grain receives a score of 1, where the plateau extends to the third signal (140°C), a score of 2 is awarded, 185°C is awarded 3, and 230°C gets 4. In this way, we are able to award every observed plateau a bleaching index score using this simple scheme. Where a single sample comprises grains that were bleached at many different times, we have the possibility to examine whether the degree of bleaching varied through time. This was the case for aeolian dune sample TW20-04 (20159) from Twigmoor Woods, and Fig. 5 shows the running mean of 5 bleaching index values,

providing a partially smoothed palaeophotometry proxy signal that spans from 18,000 to a few hundred years. We observe a striking drop during the time of the Younger Dryas, besides a series of quasi-regular cycles with a periodicity of around 1.5ka in the Holocene, possibly representing Dansgaard-Oeschger cycles (Bond et al, 2001; see Supp Mat for further discussion). At this stage we do not know what is triggering the changes in bleaching, but these might represent different transport mechanisms or rates, or variations in ground cover vegetation, for example. The authors caution against overly enthusiastic interpretation of these data, as simple random variation can produce apparently similar variations; instead, we here indicate the potential of this approach which would benefit from significantly more research.

5.0 Conclusions

In this short paper we have presented data illustrating several different ways that single grain MET-IRSL may be employed to provide valuable geomorphic information and age estimates that are accompanied by an assessment of the degree of bleaching at deposition. In each case, we consider that further developmental research will help define the scope and applicability of these approaches, and refine technical details of measurement protocols or analysis methods employed.

The successful dating using MET-IRSL for three samples from an ancient glacial context illustrates how the technique is capable of providing apparently reliable age estimates for sediments (e.g. Fig. 3), potentially similar to more thoroughly tested post-IR IRSL age determinations (e.g. Reimann et al., 2012; Kars et al., 2014; Rhodes, 2015; Rhodes and Walker, 2019; Smedley et al., 2019), as most components of the two dating systems are similar.

The MET-IRSL plateau approach can be used as a filter to isolate age estimates that relate only to meaningful bleaching events (Reimann et al., 2015; Fu and Li, 2013). Apparent ages that are simply the product of incomplete or partial bleaching of MET-IRSL signals will in general not be included in plateaux, and will automatically be excluded from further analysis within this approach, as will low values from the IR-50 signal caused by anomalous fading or adverse sensitivity change effects. This filtering action is similar to that employed as the basis of the “3ET” IRSL technique (three elevated temperatures) presented in the current issue (Ivester et al., submitted), similar to the approach of Fu and Li, 2013). In contexts where IRSL signals of grains are not fully reset while being transported within a geomorphic system, for example in highly turbid rivers, or beneath an ice sheet, multiple apparent ages

observed in sediments deposited by that system have the potential to reveal a record of past significant bleaching events within that catchment or grain population. This may provide useful information regarding grain provenance, transport history and in some cases characteristics or behaviour of the wider geomorphic system (e.g. Brown et al., 2015).

Grains that do not preserve a record of a significant bleaching event within their MET-IRSL age estimates still encode valuable information concerning their past light exposure history. This information is preserved as the burial-bleach ratio, that is, the mean gradient of the increase in age as a function of IRSL signal bleachability (Fig. 2). These signal patterns store information about repeated events over a grain's most recent environmental history. For nine samples studied and presented here, we observe an intriguing apparent relationship between the observed distribution of burial-bleach ratio and the particle size analysis (PSA) results of the sediment body (Fig. 4). We interpret this relationship as providing the first step towards attaching a measured timescale to the acquisition of PSA distributions.

When grains are exposed to light for sufficient duration effectively to bleach two or more MET-IRSL signals, information regarding the length (and/or intensity) of light exposure is encoded. This is in some ways analogous to the preservation of light exposure duration (and/or intensity) preserved by IRSL age-depth profiles in cobbles and rock surfaces (e.g. Sohbaty et al., 2012; Friesenleben et al., 2015). Here we provide an example illustrating how multiple single grains from one sediment sample can in principle provide a record of changing light exposure patterns through time (Fig. 5). This can only be achieved where certain conditions were fulfilled, specifically, grains displaying bleaching plateaux spanning a wide range of ages must be found together, as in our sample TW20-04. However, when such samples are encountered, a record of changing bleaching status through time may be constructed. Here we have chosen to present this in the form of a bleaching index where higher numbers represent better bleaching experienced at that time; in the future, it might be useful to express such records in terms of equivalent daylight exposure times. We consider that this represents a potentially interesting new environmental proxy that stores information relating to changes in landscape functioning and/or grain transport patterns.

In summary, MET-IRSL determinations applied to single grains of K-feldspar have great potential to provide information about environmental conditions pertaining at the time of deposition, or over an extended period prior to this, revealing valuable data concerning geomorphic systems (Brown, 2020).

6.0 Acknowledgements

The authors thank an anonymous reviewer for suggesting significant improvements to the manuscript, Ellie Hathaway and Rob Ashurst for field and laboratory assistance, Cathy Delaney for discussions and field visits to Chinley Brownside delta. The “Oasis in the desert?” research team is thanked for ideas and support at Ilkley Moor, in particular Graeme Swindles. We thank landowners and managers for access at Chinley, Ilkley Moor and Borrás Quarry, plus the Palglac team, in particular Christiaan Diemont, for field support and discussion of results.

7.0 References

- Bateman, M.D., Hannam, J., Livingstone, I., (1999). Late Quaternary dunes at Twiggmoor Woods, Lincolnshire, UK: a preliminary investigation. *Zeitschrift für Geomorphologie. Supplementband*, (116), pp.131-146.
- Blott, S.J., Croft, D.J., Pye, K., Saye, S.E. and Wilson, H.E., (2004). Particle size analysis by laser diffraction. *Geological Society, London, Special Publications*, 232(1), pp.63-73.
- Bond, G., Kromer, B., Beer, J., Muscheler, R., Evans, M.N., Showers, W., Hoffmann, S., Lotti-Bond, R., Hajdas, I., Bonani, G., (2001). Persistent solar influence on North Atlantic climate during the Holocene. *Science* 294, 2130–2136.
- Brown, N.D., (2020). Which geomorphic processes can be informed by luminescence measurements?. *Geomorphology*, 367, pp.107-296.
- Brown, N.D., Rhodes, E.J., Antinao, J.L., McDonald, E.V. (2015). Single-grain post-IR IRSL signals of K-feldspars from alluvial fan deposits in Baja California Sur, Mexico. *Quaternary International* 362, 132-138, <http://dx.doi.org/10.1016/j.quaint.2014.10.024>
- Chiverrell, R.C., Thomas, G.S.P., Burke, M., Medialdea, A., Smedley, R., Bateman, M., Clark, C., Duller, G.A.T., Fabel, D., Jenkins, G., Ou, X., Roberts, H.M., Scourse, J. (2020). The evolution of the terrestrial-terminating Irish Sea glacier during the last glaciation. *Journal of Quaternary Science* 36, 752-779.

- Colarossi, D., Duller, G. A. T., Roberts, H. M. (2018). Exploring the behaviour of luminescence signals from feldspars: implications for the single aliquot regenerative dose protocol. *Radiation Measurements*, 109, 35-44.
- Dansgaard, W., White, J.W.C. and Johnsen, S.J., (1989). The abrupt termination of the Younger Dryas climate event. *Nature*, 339(6225), pp.532-534.
- Delaney, C.A., Rhodes E.J., Crofts, R.G., Jones, C.D. (2010). Evidence for former glacial lakes in the High Peak and Rossendale Plateau areas, north west England. *North West Geography* 10, 1-17.
- Freiesleben, T., Sohbaty, R., Murray, A., Jain, M., Khasawneh, S., Hvidt, S., Jakobsen, B., (2015). Mathematical model quantifies multiple daylight exposure and burial events for rock surfaces using luminescence dating. *Radiation Measurements* 81, 16-22.
- Fu, X., Li, S.H. (2013). A modified multi-elevated-temperature post-IR IRSL protocol for dating Holocene sediments using K-feldspar. *Quaternary Geochronology* 17, 44-54, <http://dx.doi.org/10.1016/j.quageo.2013.02.004>
- Gale, S.J., Hoare, P.G. (2011). *Quaternary sediments: petrographic methods for the study of unlithified rocks*. Second edition. Caldwell, N.J., Blackburn.
- Gray, H.J., Tucker, G.E., Mahan, S.A., McGuire, C., Rhodes, E.J., (2017). On extracting sediment transport information from measurements of luminescence in river sediment. *Journal of Geophysical Research: Earth Surface*, 122(3), pp.654-677.
- Guo, Y., Li, B., Zhao, H. (2020) Comparison of single-aliquot and single-grain MET-pIRIR De results for potassium feldspar samples from the Nihewan Basin, northern China. *Quaternary Geochronology* 56, 101040 <https://doi.org/10.1016/j.quageo.2019.101040>
- Ivester, A.H., Rhodes, E.J., Dolan, J.F., Van Dissen, R.J., Gauriau, J., Little, T., McGill, S.F., Tuckett, P.A. A method to evaluate the degree of bleaching of IRSL signals in feldspar: The 3ET method. *Quaternary Geochronology* (submitted, this volume).

- Jowett, A., Charlesworth, J.K. (1929). The glacial history of the Derbyshire dome and the western slopes of the southern Pennines. *Quarterly Journal of the Geological Society of London*, 85, 307-334.
- Kars, R.H., Reimann, T., Wallinga, J. (2014). Are feldspar SAR protocols appropriate for post-IR IRSL dating? *Quaternary Geochronology* 22, 126-136, <http://dx.doi.org/10.1016/j.quageo.2014.04.001>
- King, G.E., Herman, F., Lambert, R., Valla, P.G., Guralnik, B., (2016). Multi-OSL-thermochronometry of feldspar. *Quaternary Geochronology* 33, 76-87.
- Lamothe, M., Auclair, M., Hamzaoui, C., Huot, S., 2003. Towards a prediction of long-term anomalous fading of feldspar IRSL. *Radiation Measurements* 37, 493–498, doi:10.1016/S1350-4487(03)00016-7
- Li, B., Li, S.H., (2011). Luminescence dating of K-feldspar from sediments: a protocol without anomalous fading correction. *Quaternary Geochronology*, 6(5), pp.468-479.
- Li, B., Jacobs, Z., Roberts, R.G., Li, S.H., (2014). Review and assessment of the potential of post-IR IRSL dating methods to circumvent the problem of anomalous fading in feldspar luminescence. *Geochronometria*, 41(3), pp.178-201.
- López, G.I., (2017). Grain size analysis. *Encyclopedia of Geoarchaeology [Internet]*. Dordrecht: Springer Netherlands, pp.341-8.
- McGuire, C.P., Rhodes, E.J. (2015a). Determining fluvial sediment virtual velocity on the Mojave River using K-feldspar IRSL: Initial assessment. *Quaternary International*, 362, 124–131.
- McGuire, C.P., Rhodes, E.J., (2015b). Downstream MET-IRSL single-grain distributions in the Mojave River, southern California: Testing assumptions of a virtual velocity model. *Quaternary Geochronology*, 30, 239-244.
- Reimann, T., Thomsen, K.J., Jain, M., Murray, A.S., Frechen, M. (2012). Single-grain dating of young sediment using the pIRIR signal from feldspar. *Quat. Geochronol.* 11,

28–41. <https://doi.org/10.1016/j.quageo.2012.04.016>

- Reimann, T., Notenboom, P. D., De Schipper, M. A., Wallinga, J. (2015). Testing for sufficient signal resetting during sediment transport using a polymineral multiple-signal luminescence approach. *Quaternary Geochronology*, 25, 26-36.
- Rhodes, E.J., (2015). Dating sediments using potassium feldspar single-grain IRSL: initial methodological considerations. *Quaternary International*, 362, pp.14-22.
- Rhodes, E.J., Walker, R.T., (2019). Applications of luminescence dating to active tectonic contexts. In: *Handbook of luminescence dating* (Bateman, M.D. ed.). Whittles publishing, Caithness, 293-320.
- Rui, X., Zhang, J.F., Hou, Y.M., Yang, Z.M., Liu, Y., Zhen, Z.M., Zhou, L.P. (2015). Feldspar multi-elevated-temperature post-IR IRSL dating of the Wulanmulun Paleolithic site and its implication. *Quaternary Geochronology* 30, 438-444, <http://dx.doi.org/10.1016/j.quageo.2015.05.004>
- Smedley, R.K., Buylaert, J.P., Ujvari, G. (2019). Comparing the accuracy and precision of luminescence ages for partially-bleached sediments using single grains of K-feldspar and quartz. *Quaternary Geochronology* 53, 101007,
- Smedley, R.K., Duller, G.A.T. (2013). Optimising the reproducibility of measurements of the post-IR IRSL signal from single-grains of feldspar for dating. *Anc. TL* 31 (2), 49–58.
- Smedley, R.K., Duller, G.A.T., Roberts, H.M., (2015). Assessing the bleaching potential of the post-IR IRSL signal for individual K-feldspar grains: implications for single-grain dating. *Radiat. Meas.* 79, 33–42.
- Sohbati, R., Murray, A.S., Chapot, M.S., Jain, M., Pederson, J., (2012). Optically stimulated luminescence (OSL) as a chronometer for surface exposure dating. *J. Geophys. Res.* 117, B09202. <https://doi.org/10.1029/2012JB009383>.
- Sun, D., Bloemendal, J., Rea, D.K., Vandenberghe, J., Jiang, F., An, Z., Su, R., (2002). Grain-size distribution function of polymodal sediments in hydraulic and aeolian

environments, and numerical partitioning of the sedimentary components. *Sedimentary geology*, 152(3-4), pp.263-277.

Zinke, R., Dolan, F.D., Rhodes, E.J., Van Dissen, R., McGuire, C.P., (2017). Lidar and luminescence dating analysis reveals highly variable latest Pleistocene–Holocene slip rates on the Awaterere fault at Saxton River, South Island, New Zealand. *Geophysical Research Letters*, 44, <https://doi.org/10.1002/2017GL075048>

Table captions

Table 1. Multiple elevated temperature IRSL single aliquot regenerative-dose (SAR) protocol used in this study, based on McGuire and Rhodes (2015b).

Table 2. Details of combined equivalent doses, dose rates and age estimates for three samples of an ice-marginal glacial delta from Chinley Brownside, Derbyshire, UK. Note the expected age from independent dating of the British and Irish Ice Sheet (BIIS) is in the range 24-28ka.

Figure Captions

Fig. 1. Three different types of MET-IRSL responses. These comprise a) Plateau response, here shown by the consistency of the lowermost three MET-IRSL measurements, indicated by the fine dashed line; b) Rising response, spanning the full MET range; the slope of the dashed line has a relationship to the burial-bleach (B-B) ratio described in the main text; c) Anomalous response, showing out of order apparent age estimates.

Fig. 2. Apparent age vs characteristic bleach time for the MET-IRSL signals of two different K-feldspar grains from sample TW20-04 Shfd 20159. The upper sample (blue in colour version) has a steep gradient while the lower sample (red in colour version) has a low gradient. The gradients of these fits provide the burial-bleach ratio (B-B ratio).

Fig. 3. MET-IRSL plateau age estimates for three samples from an ice-marginal glacial delta located in Chinley Brownside, Derbyshire, UK. Grains measured were 125-180 μ m except for subsample 16132b which used the 180-212 μ m fraction. Only the lowermost age estimates for each sample are shown, in increasing age order. Results displayed as solid symbols (red in colour image) are included in each age estimate, isolated using the statistical approach

described by Rhodes (2015); the combined age for each is indicated by the dashed line and the value displayed on the plot in ka with the associated 1 sigma uncertainties.

Fig. 4. Comparison of particle size analysis (PSA) results from different sample (left plots) with distributions of burial-bleach (B-B) ratio values (right plots). Sample field and laboratory codes are shown on plots. PSA results are shown for standard grain size distributions, indicated by letters at the bottom of the figure; these stand for the following: c = clay, vfsi = very fine silt, fsi = fine silt, msi = medium silt, csi = coarse silt, vfs = very fine sand, fs = fine sand, ms = medium sand, cs = coarse sand, vcs = very coarse sand, g = granules, p = pebbles. We note a similarity in the widths and positions of distributions in some cases, in particular for the upper six samples from controlled sedimentary environments. Results to the right of the plots may represent higher energy transport and depositional conditions with coarser sediment grades and steeper (greater) B-B ratios. See text for further details.

Fig. 5. A partially smoothed palaeophotometry proxy signal based on the running mean of 5 bleaching index values from different single grain plateau age estimates of sample TW20-04, laboratory code Shfd 20159, ranging from 18,000 years ago until a few hundred years ago. We observe a striking drop during the time of the Younger Dryas, besides a series of quasi-regular cycles with a periodicity of around 1.5ka in the Holocene, possibly representing Dansgaard-Oeschger cycles. See text for further details and caveat regarding interpretation of these data.

Table 1. Multiple elevated temperature IRSL single aliquot regenerative-dose (SAR) protocol used in this study, based on McGuire and Rhodes (2015b).

Step	Each SAR MET-IRSL cycle comprises:
1	Natural or laboratory beta dose
2	Preheat 60s 250°C 5°Cs ⁻¹
3	SG IRSL 50°C 2.5s 90% power
4	SG IRSL 95°C 2.5s 90% power
5	SG IRSL 140°C 2.5s 90% power
6	SG IRSL 185°C 2.5s 90% power
7	SG IRSL 230°C 2.5s 90% power
8	Beta test dose 8 Gy
9	Preheat 60s 250°C 5°Cs ⁻¹
10	SG IRSL 50°C 2.5s 90% power
11	SG IRSL 95°C 2.5s 90% power
12	SG IRSL 140°C 2.5s 90% power
13	SG IRSL 185°C 2.5s 90% power
14	SG IRSL 230°C 2.5s 90% power
15	MG IRSL Hot Bleach 290°C 100s 90% power

Table 2. Details of combined equivalent doses, dose rates and age estimates for three samples of an ice-marginal glacial delta from Chinley Brownside, Derbyshire, UK. Note the expected age from independent dating of the British and Irish Ice Sheet (BIIS) is in the range 24-28ka.

Field code	Lab code	Grain size (μm)	Equivalent dose ± 1 sigma (Gy)	Sed. K conc. (%)	Sed. Th conc. (ppm)	Sed. U conc. (ppm)	Gamma dose rate ± 1 sigma (mGya^{-1})	Total dose rate ± 1 sigma (mGya^{-1})	MET-IRSL age ± 1 sigma (mGya^{-1})
BS16-01	Shfd16132	125-180	51.17 ± 2.66	1.10	4.30	1.25	0.697 ± 0.014	2.19 ± 0.11	23.4 ± 1.7
BS16-01	Shfd16132	180-212	50.22 ± 2.36	1.10	4.30	1.25	0.697 ± 0.014	2.32 ± 0.11	21.7 ± 1.5
BS16-02	Shfd16133	125-180	49.57 ± 2.99	1.30	5.40	1.57	0.704 ± 0.015	2.35 ± 0.13	21.1 ± 1.7
BS16-03	Shfd16134	125-180	59.29 ± 3.26	1.40	7.10	1.93	0.711 ± 0.015	2.48 ± 0.14	23.9 ± 1.9

Fig. 1

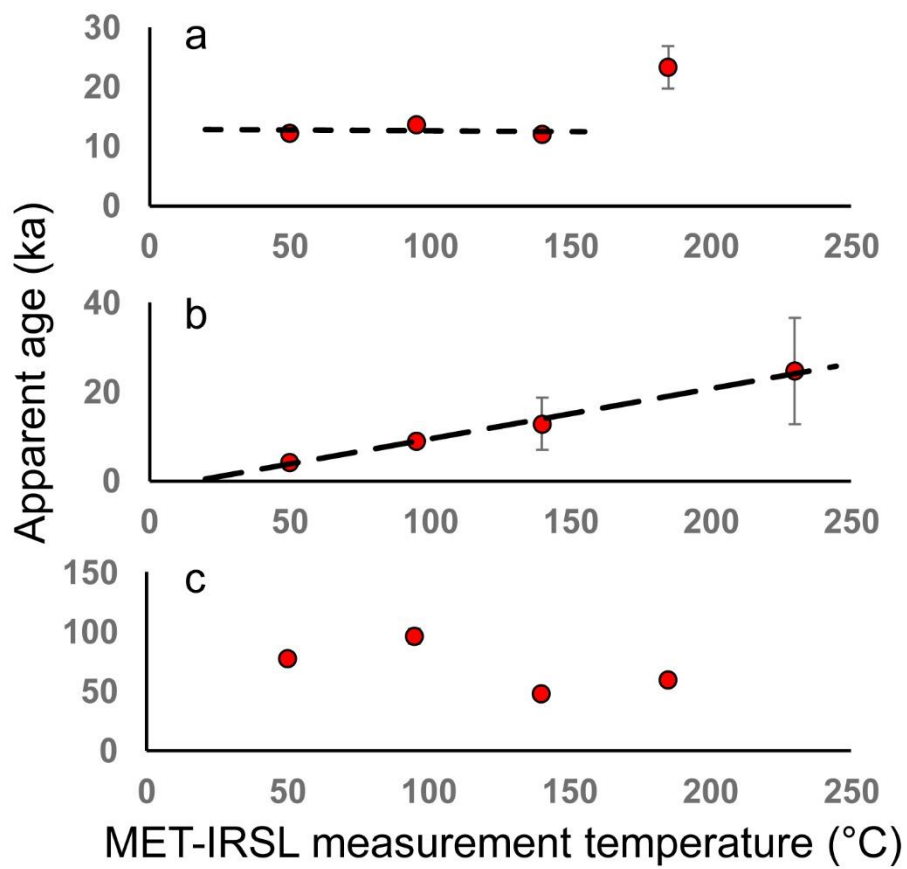


Fig. 1. Three different types of MET-IRSL responses. These comprise a) Plateau response, here shown by the consistency of the lowermost three MET-IRSL measurements, indicated by the fine dashed line; b) Rising response, spanning the full MET range; the slope of the dashed line has a relationship to the burial-bleach (B-B) ratio described in the main text; c) Anomalous response, showing out of order apparent age estimates.

Fig. 2

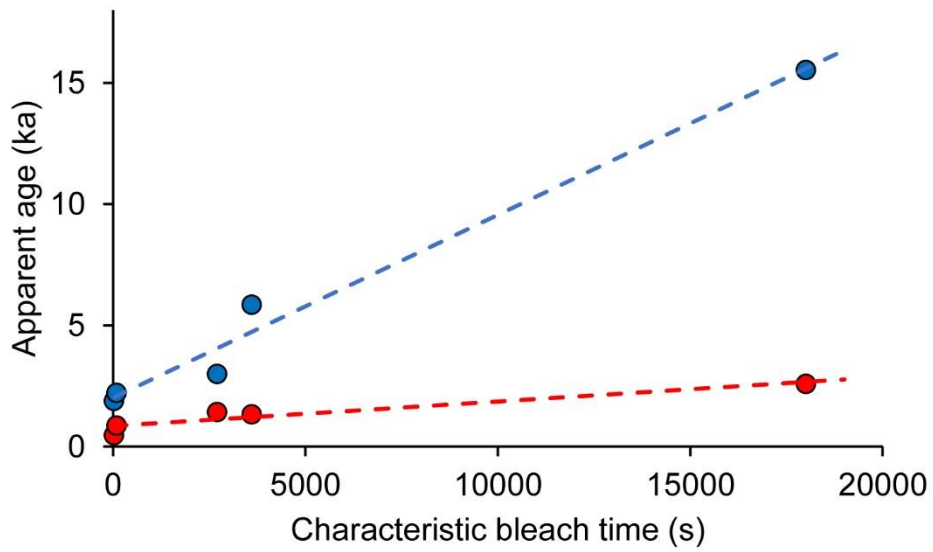


Fig. 2. Apparent age vs characteristic bleach time for the MET-IRSL signals of two different K-feldspar grains from sample TW20-04 Shfd 20159. The upper sample (blue in colour version) has a steep gradient while the lower sample (red in colour version) has a low gradient. The gradients of these fits provide the burial-bleach ratio (B-B ratio).

Fig. 3

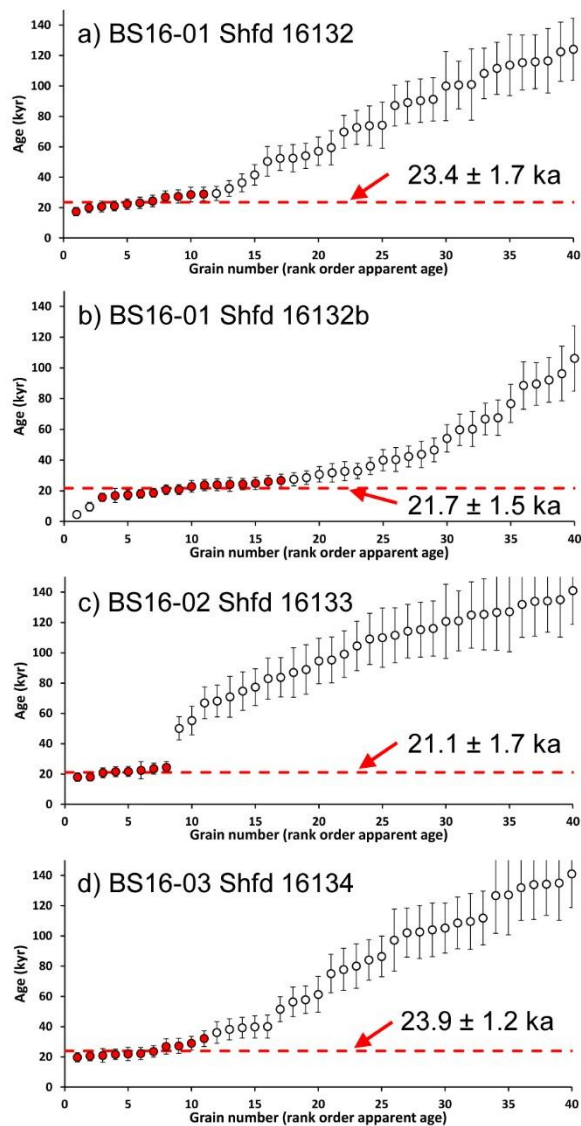


Fig. 3. MET-IRSL plateau age estimates for three samples from an ice-marginal glacial delta located in Chinley Brownside, Derbyshire, UK. Grains measured were 125-180 μ m except for subsample 16132b which used the 180-212 μ m fraction. Only the lowermost age estimates for each sample are shown, in increasing age order. Results displayed as solid symbols (red in colour image) are included in each age estimate, isolated using the statistical approach described by Rhodes (2015); the combined age for each is indicated by the dashed line and the value displayed on the plot in ka with the associated 1 sigma uncertainties.

Fig. 4

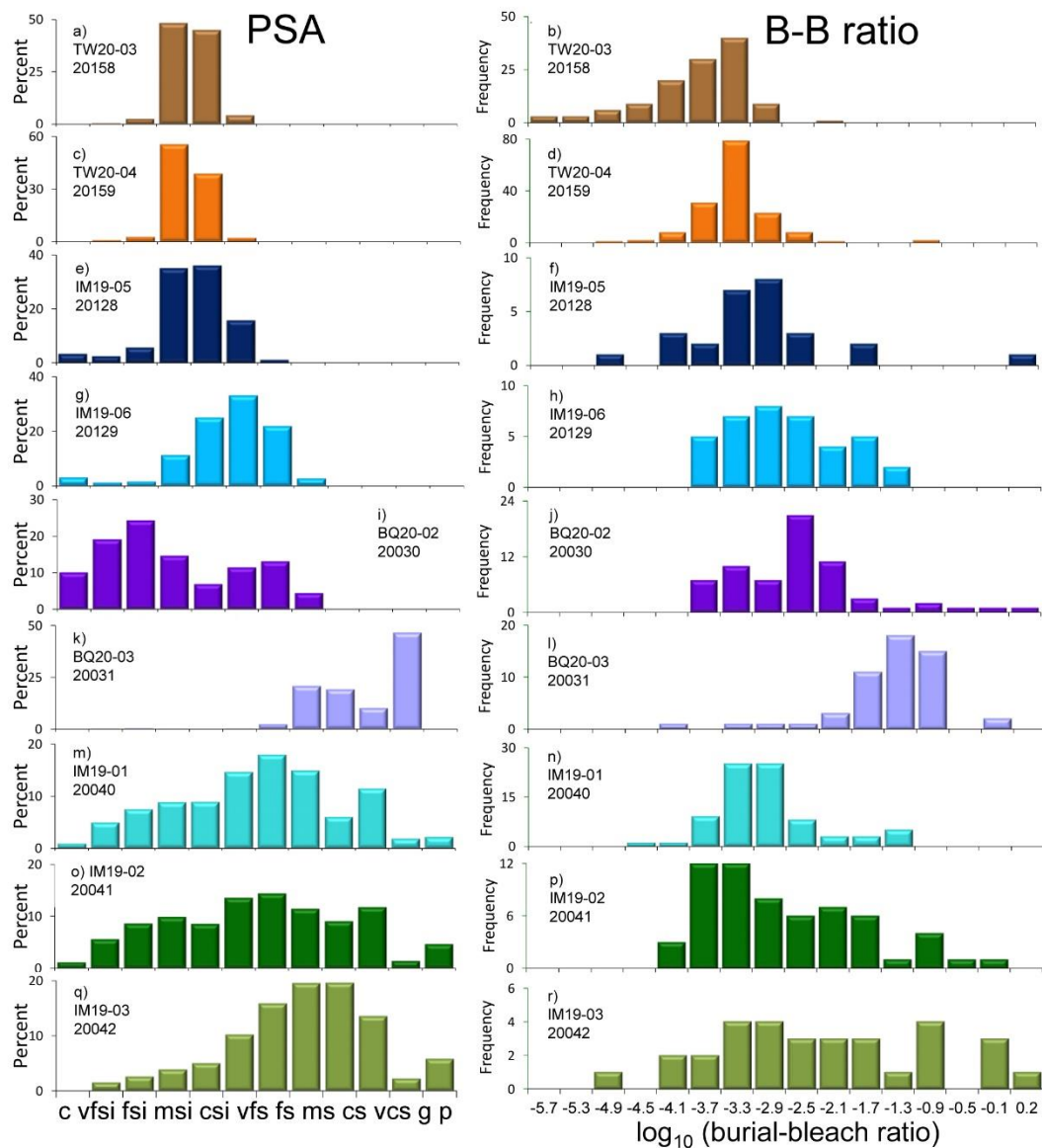


Fig. 4. Comparison of particle size analysis (PSA) results from different sample (left plots) with distributions of burial-bleach (B-B) ratio values (right plots). Sample field and laboratory codes are shown on plots. PSA results are shown for standard grain size distributions, indicated by letters at the bottom of the figure; these stand for the following: c = clay, vfsi = very fine silt, fsi = fine silt, msi = medium silt, csi = coarse silt, vfs = very fine sand, fs = fine sand, ms = medium sand, cs = coarse sand, vcs = very coarse sand, g = granules, p = pebbles. We note a similarity in the widths and positions of distributions in some cases, in particular for the upper six samples from controlled sedimentary environments. Results to the right of the plots may represent higher energy transport and depositional conditions with coarser sediment grades and steeper (greater) B-B ratios. See text for further details.

Fig. 5

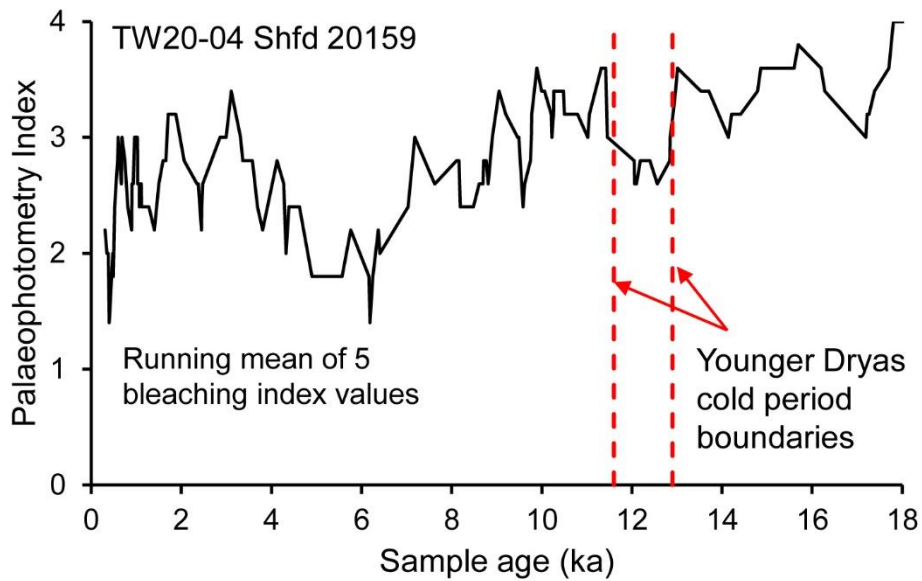


Fig. 5. A partially smoothed palaeophotometry proxy signal based on the running mean of 5 bleaching index values from different single grain plateau age estimates of sample TW20-04, laboratory code Shfd 20159, ranging from 18,000 years ago until a few hundred years ago. We observe a striking drop during the time of the Younger Dryas, besides a series of quasi-regular cycles with a periodicity of around 1.5ka in the Holocene, possibly representing Dansgaard-Oeschger cycles. See text for further details and caveat regarding interpretation of these data.